Coupled CFD and structural analysis for world outright sailing speed record preparations

T Clarke and S Howell, Verney Yachts, UK

Andrey Aksenov, Igor Moskalev, Konstantin Kuznetsov, CAPVIDIA, Russia

Abstract: The brief for the boat, v-39 Albatross is to set a new world outright sailing speed record at Portland Harbor, UK by 2013. The boat is configured to add at least 10 knots to the current record by setting a speed above 65 knots (120 km/h). At speed the boat hulls will fly above the surface using a wing in ground effect. The pilot is able to sail on both port and starboard tack and can actively control the craft in speed, roll and height as well as direction.

Verney Yachts and Capvidia are carrying out transient Fluid Structure Interaction (FSI) simulations using Abaqus/Standard coupled with FlowVision-HPC from Capvidia. The objectives of the simulations described in this paper are to capture the above surface aerodynamics of the boat, and to establish overall aerodynamic forces and moments acting on the boat with different control inputs and boat speeds. Each FSI analysis involves capturing the movement of six independently rotating surfaces (four wing-sail surfaces and two outriggers), each surface able to freely weathervane into the local airflow. This process allows the control system to be tuned to minimize control cross coupling and to maximize forward thrust, whilst maintaining roll balance of the overall boat.

The work presented herein is being carried out alongside Computational Fluid Dynamics (CFD) analyses of the free surface hydrodynamics. The data generated will be pulled together into a final series of mathematical models to plot and analyze the forces and moments acting on the boat as the speed increases, mapping the way the boat will behave.

Keywords: CFD, Computational Fluid Dynamics, Transient, Coupled, Fluid-Structure Interaction, Speed Sailing, Sailing Speed Record, Wing-Sails, Wing In Ground Effect.

1. Introduction

1.1 Background

The work described herein is part of a wider project to design and build a sailing boat, v-39 Albatross to challenge the current world outright sailing speed record. An outright speed record attempt involves sailing a straight course of 500m without the use of powered control systems. As the work began, the project was moving from a conceptual to preliminary phase. At this stage the aerodynamic, hydrodynamic and hydrostatic forces and moments acting on the boat, across the speed range, needed to be understood with a greater level of fidelity. As the work progresses, further optimization of the boat shape, mass properties and control system can take place.

1.2 Conceptual design

The overall concept of the boat involves providing a single crew member or pilot with a degree of active control which compares to that provided to a pilot of a glider or sailplane. At speed, the boat hulls rise free of the water surface through aerodynamic lift generated by a wing in ground effect. Once the hulls are free of the surface, the pilot is able to actively control the boat in roll, height and yaw. The high degree of active control enables the pilot to maintain the hulls free of the surface for prolonged periods of time. In this configuration, only a single keel and rudder with 'T' hydrofoil is penetrating the surface. The maximum speed of the boat is restricted only by the incipient cavitation speed of the keel and rudder surfaces. Since the pilot is able to actively control the height of the boat above the surface, he is in effect controlling the depth of penetration of the keel and rudder into the water. Since these surfaces form the largest contributors to the overall drag of the boat, actively controlling the height of the boat is an active form of speed control. This process enables the pilot to maintain a boat speed close to the incipient cavitation speed of the underwater foils for prolonged periods when the boat is subjected to a range of true wind speeds.

The boat is presented in Figure 1. The boat can sail on both port and starboard tack. It tacks by rolling through 90 degrees as it turns through the wind; the hull forward section rotates between two fixed positions to remain upright. The vertical sail becomes the horizontal wing and the horizontal wing becomes the vertical sail as the boat tacks. The hull aft section has fixedly mounted to it the two wing-sails, the two keels and the two rudders. When the boat tacks, transposing of keels takes place, enabling the use of a cambered section. The use of camber increases the performance of the keel.

Table 1. Specification for v-39.

Velocity not to exceed (incipient cavitation):	70 knots (80.5 mph, 129.6 km/h)
Target lift / drag ratio:	2.3:1
Overall length:	39 feet (11.9m)
Sail area:	26 m2 (52 m2 for both wing-sails)
Mass including pilot & ballast:	650 kg

Each wing-sail of v-39 is split into an inner and outer plank (four planks in total), as shown in Figure 2. Each plank is free to rotate or 'weathervane' about its longitudinal axis into the local air stream. In addition, each plank is aerodynamically and mass balanced about its axis of rotation. Similarly, each outrigger is free to rotate about the same axis described above. When an outrigger is not in contact with the water, it simply weathervanes (aligns) into the local air stream. It is important to note that each plank and each outrigger is free to independently rotate about its axis, with only aerodynamic influences between them. The pilot has no direct control over the planks or the outriggers. For each of the four planks, the angle of attack relative to the local air stream is determined by the degree of flap deflection at the trailing edge, over which the pilot does have control.

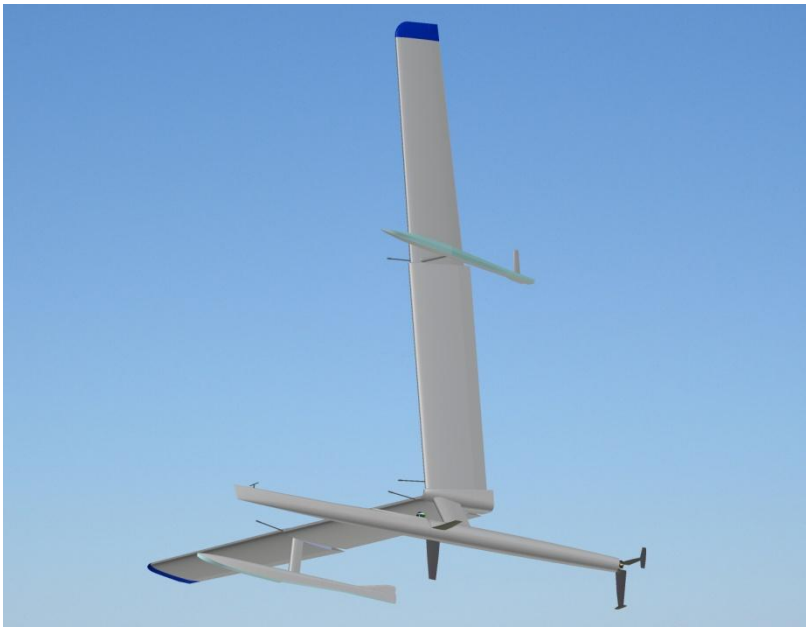

Figure 1. v-39 perspective.

Referring to the cross-section through the wing sail (Figure 2), with zero flap deflection, a plank produces zero lift. Increasing upward deflection of a given flap induces increasing lift from the plank, up to the stalling point of the airfoil.

This aerodynamic characteristic is achieved by careful design of the plank airfoil section. The section is designed to have a zero pitching moment with zero flap deflection and an increasing positive pitching moment with increasing negative (upward) flap deflection. The position of the axis of rotation is important and is stationed at approximately 22% chord.

The pilot has directional control of the boat by operating rudder pedals with his feet. He also has a control stick which, if pulled backward, increases the upwards deflection of each trailing edge flap and therefore increases the lift generated by each of the planks. Moving the stick fore to aft gives the pilot control of the speed of the boat when the hulls remain in the water. When the hulls lift free from the water, moving the stick fore to aft controls the height of the boat above the surface and therefore controls the speed by setting the amount of keel in the water. Moving the stick left to right gives the pilot roll control of the boat. This is achieved by moving all four trailing edge flaps, each in the opposite sense to its neighbouring flap, to effectively shift the spanwise lift distribution of each wing-sail, without transferring overall lift from one wing-sail to the other. This will minimise any lift/roll cross coupling effects.

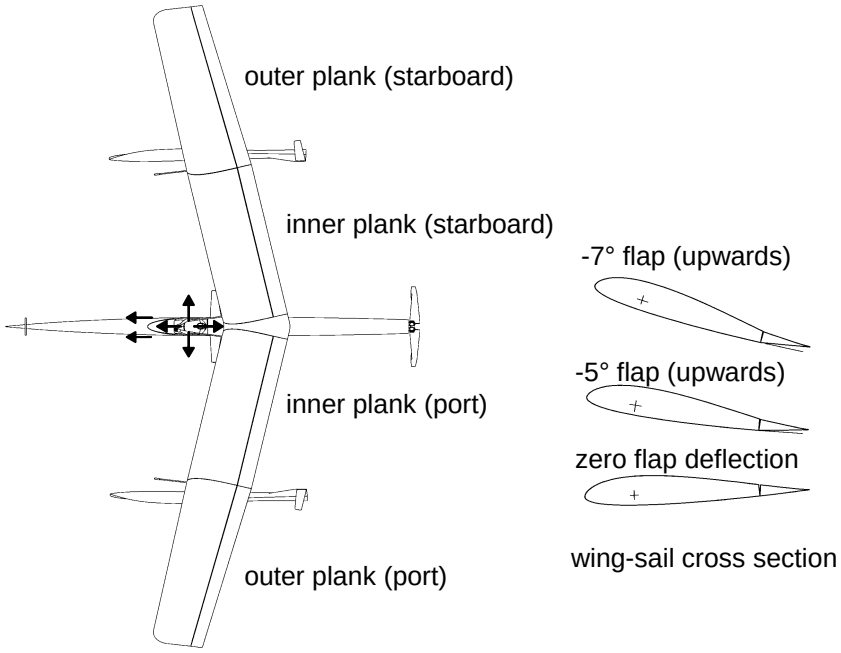

Figure 2. v-39 wing-sail planks and movement of controls.

1.3 Scope

At a given boat speed, all of the external forces acting on the boat need to be predicted. These include aerodynamic, hydrodynamic and at lower speeds with the hulls in contact with the water, hydrostatic forces. A computational approach has been chosen to generate the fluids data necessary to complete this work. For simplification of the process, simulations have been split into three groups: aerodynamics, hull hydrodynamics/hydrostatics and finally foil hydrodynamics. The data generated for each of the three groups of analyses can be pulled together into a final series of mathematical models to build a complete picture of the boat's performance, stability and control.

The work described within this paper covers preliminary work for the first group of analyses, to capture the aerodynamic characteristics of the boat. This has led to the development of a transient coupled CFD and structural analysis of the entire above surface structure within a single computational domain. Before a simulation can be run, conditions need to be set and will remain fixed during a run, which includes the position of each control surface, boat speed, wind speed, gradient and direction. Once running, a simulation will capture the rotational movement of each of the four wing-sail planks and each outrigger. Each of the six surfaces is able to self-align under the influence of the airflow, or weathervane about its axis of rotation, with near zero mechanical interaction between them. However, each rotating surface will exert an aerodynamic influence over each of the other surfaces. The principle results for each run are the resultant forces and moments in relation to a chosen coordinate system.

The results presented in this paper focus on the lift force generated for a range of flap deflections. Comparisons are drawn between these results and the predicted lift force versus flap deflection from the concept design study described in section 1.4 below. A simulation may show any unsteady flow giving rise to oscillating movements of the wing-sail planks, which has also been investigated within this study.

1.4 The requirement for coupled CFD and structural analysis

During the concept design phase, aerodynamic and hydrodynamic characteristics of the lifting surfaces were predicted by a process of 2D analysis of the lifting surface airfoil section using X-foil (an analysis and design code for low Reynolds number airfoils) and 3D wing analysis using the discrete vortex Weissinger computation method. Empirical data was used for the prediction of the lift and drag associated with the hulls. It was realized, at this early stage, the limitations associated with such an approach. The airflow around the craft is complex and could be likened to the flow around an aircraft whilst flying with a very high degree of sideslip. One such limitation is the 3D wing analysis carried out assumed continuous twisting of the wing-sail; however, in reality, wing twist is provided by splitting each wing-sail into two discrete surfaces (planks) and rotationally displacing one from the other, thereby creating a discontinuity between the two surfaces.

It was also understood that the close coupled static stability of the 'tailless' wing-sail planks could be easily upset by undesired fluid structure interactions.

Fluids data needed to be captured with a greater level of detail to further investigate the characteristics of the overall sail-boat concept, and to further optimize the boat shape, mass properties and control system. Since each wing-sail plank is freely rotating and exhibits a closely coupled balance of forces, it was understood that a coupled fluids analysis with structural analysis needed to be developed to provide realistic results.

2. Fluid-structure interactions for the wing-sail

The analyses have been split into two groups: single degree of freedom wing-sails (with each plank only rotating about its longitudinal axis); and fully deformable wing-sails with the axis of each wing sail allowed to deform under the predicted aerodynamic loads.

2.1 Single degree of freedom wing-sails

The adopted aerodynamic design makes it necessary for each plank to mimic the behavior of a tubular or axisymmetric structure centered at the axis of rotation. A tubular structure, or one which behaves as such, which is free to rotate about its longitudinal axis, has no motive to rotate under bending loads. This requirement is essential to preserve the close coupled aerodynamic balance of the wing-sails. Since the structure of each plank has been carefully designed to provide this characteristic, it is possible to assume that each plank is unable to deform under load. The extent of structural coupling within an analysis can therefore be simplified down to capturing the rotational movement of each plank and each outrigger.

The unloaded angle between each wing-sail is set to be greater than 90 degrees. When loaded and supporting the full weight of the boat, the angle between each wing-sail is approximately 90

degrees. For the preliminary cases presented herein, it was assumed that the wing-sails are not deformed and are separated from each other by 90 degrees, as given in Figure 3 below.

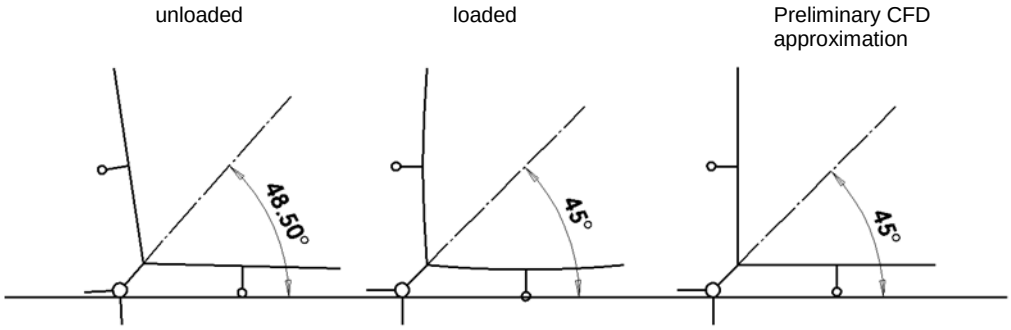

Figure 3. Wing-sail deflection.

2.2 Fully deformable wing-sails

A detailed Abaqus FE model of the wing-sail has been constructed which has been used to predict the structural characteristics of the wing-sail [1]. A further simplified FE model of the wing-sail has been constructed and correlated with the detailed model, such as to give a similar overall structural behavior, although local deformations of the wing-sail skin is not captured at this stage. This simplified FE model is being used as part of a series of ongoing fluid structure interaction analyses to capture the aerodynamic characteristics of the boat in which the deformation of each wing-sail along its axis is also captured.

3. A statement of the problem

A boat speed of 20.58 m/s (74 km/h) is taken for the simulations described in this paper. Each simulation is carried out in a frame reference relative to the boat. This means the boat is fixed in a computational domain and air flows around it with relative speed. The wind speed is non-uniform along the vertical axis to take into account a wind boundary layer near the sea surface.

The boat as an Abaqus finite-element mesh is submerged into a computational domain. The computational domain is specified as a box with dimensions 90m x 70m x 45m. The bottom of the box represents a still surface of the sea: disturbing of the water surface is not yet simulated.

Apparent wind enters the computational domain on two box faces (inlet faces) and exits from two outlet faces, as shown in Figure 4. A pressure boundary condition is specified on the outlet faces and total pressure condition on the inlet faces. A boundary condition with a logarithmic wall function is specified over all boat surfaces.

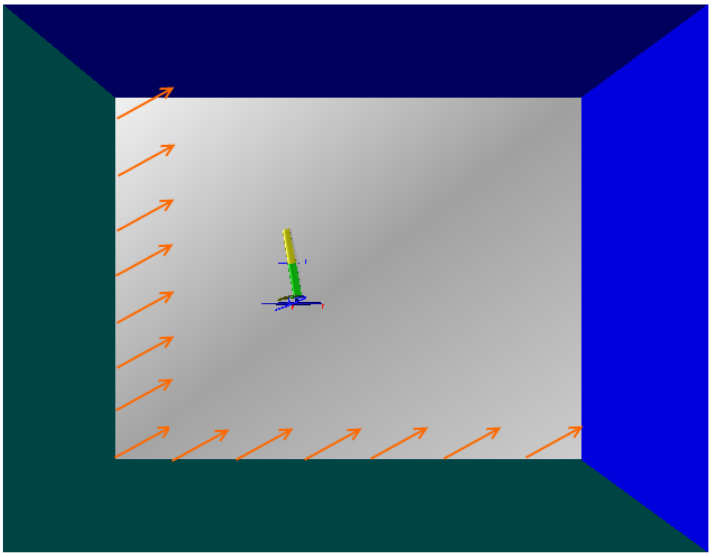

Figure 4. CFD computational domain (looking downward).

4. Computational model

4.1 Finite element model of the boat

From the assumptions stated in section 2.1, each wing-sail plank should not deform under wind loads. Thus, the statement of the problem in Abaqus is reduced to modeling the motion of boat parts as absolutely rigid bodies. To realize this model in Abaqus, every part of the boat is assumed to be rigid and all interactions between the pieces are idealized with node-to-node interactions.

Discrete rigid body representation is used within Abaqus for the FSI simulations, since it allows the import of hydrodynamic forces from FlowVision into Abaqus as nodal forces. This type of rigid body is assigned to the geometry of each movable part of the boat. To determine the inertial characteristics of each part, the local coordinate system and the reference point coinciding with its centre, are assigned to the parts (Figure 5).

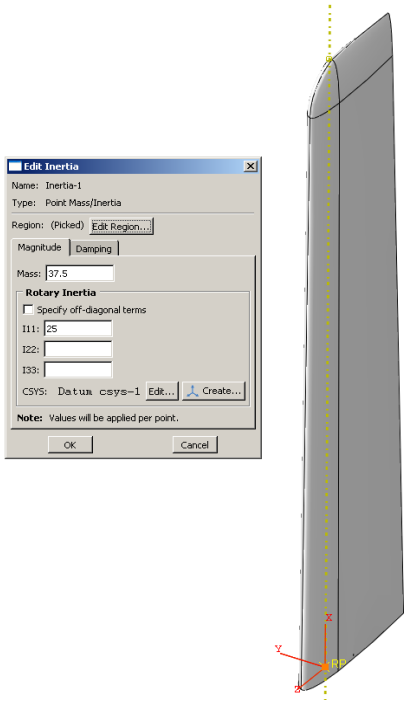

Figure 5. Outer wing-sail plank in Abaqus.

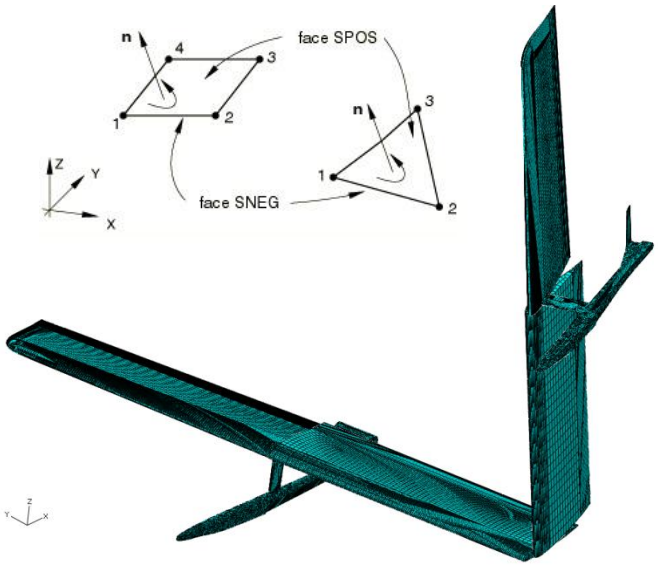

Figure 6. Finite-element model of wing-sail structure.

The finite-element model of the wing-sail structure is shown in Figure 6. It includes four planks complete with trailing-edge flaps and two outriggers. Each flap is fixed at a chosen angle with respect to its associated plank at the start of each simulation and then moves with the plank as one body for the course of that simulation. The model consists of 210,490 three dimensional rigid elements of type R3D4 and R3D3, which allows the export of pressure via Abaqus Direct Coupling Interface as nodal forces which are uniformly distributed over the surfaces. To specify rotation of the boat's moving parts only around prescribed axes, Connector / Hinge two-node elements are used as annotated in Figure 6.

4.2 CFD model

The CFD mesh in FlowVision is built fully automatically using the Subgrid Geometry Resolution method. To take into account peculiarities of computational domain shape, motion of the moving parts or solution, the mesh is adapted by using local adaptation techniques. These techniques allow small details of the boat's shape to be resolved without large increases of the number of cells. During adaptation each cell is divided into 8 smaller cells. Each division is designated by a level number; the highest level belongs to the smallest cells. The number of levels is unlimited in FlowVision.

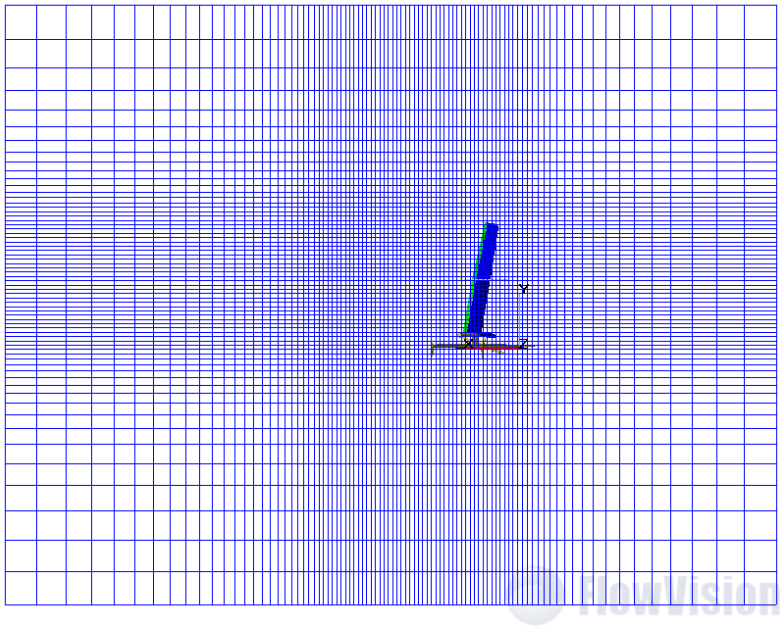

Figure 7. Initial CFD grid.

The non-uniform initial grid (adaptation level=0), which comprised around 400 000 cells is shown in Figure 7. The grid near the boat is adapted in volumes and over surfaces. Volumetric adaptation near the wing-sails with level=1 is shown in Figure 8. Adaptation level=4 is used to refine mesh near each wing surface (Figure 9). Also, experience gained from wing simulations and grid convergence analyses shows that it is necessary to further resolve the grid around each wing-

sail leading edge and over the surface of each flap. To meet these requirements, the grid is adapted at the wing leading edge with level=5 as shown in Figure 9.

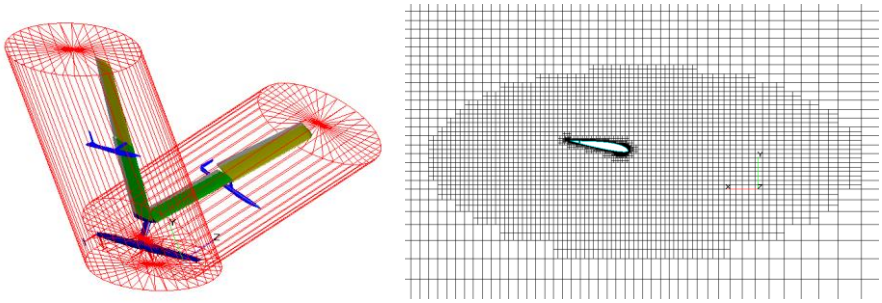

Figure 8. Volume adaption around wing-sails.

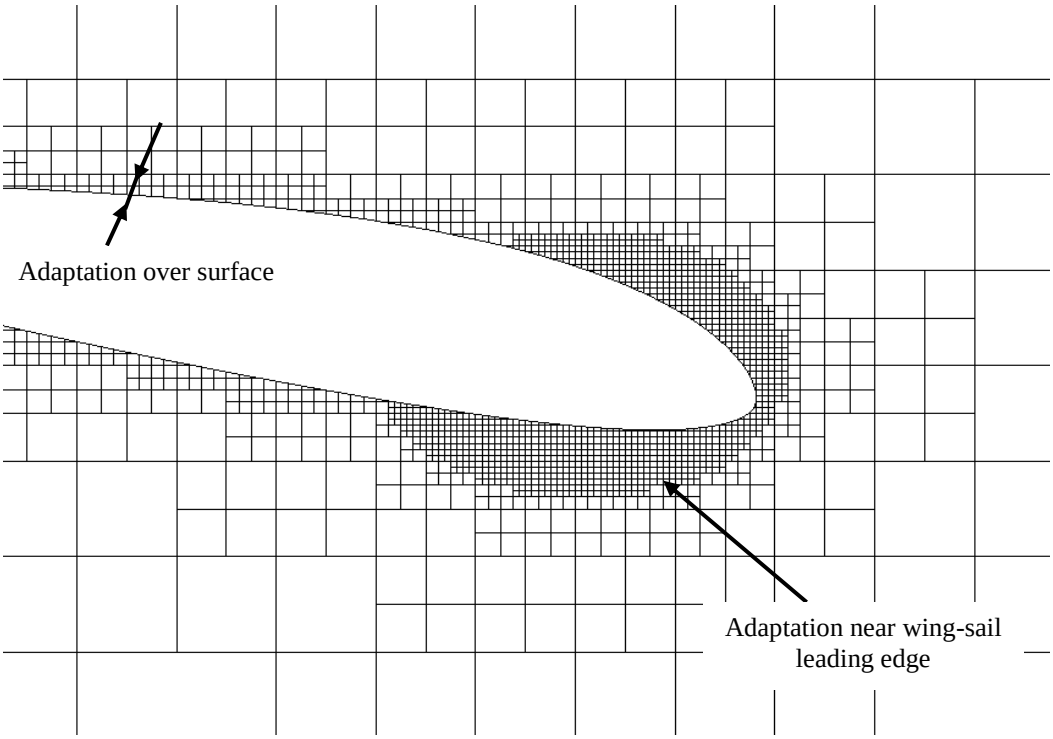

Figure 9. Grid adaptation near wing surface.

A series of grid convergence analyses were undertaken to investigate the reliability of the CFD simulation results, and the predicted wing lift and boat roll moment as a function of mesh cell count for a typical case, the result of which is shown in Figure 10. It is apparent that as the CFD mesh is refined beyond a cell count of 4 million cells, the influence of mesh refinement upon the predictions becomes less important. All results given within this paper use a grid with 8 million cells.

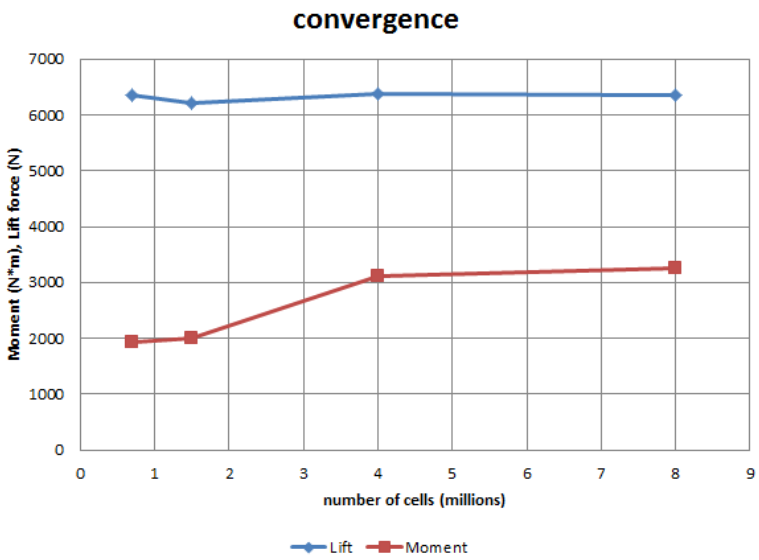

Figure 10. Wing-sail lift and roll moment as a function of CFD mesh cell count.

4.3 Co-simulation

The co-simulation analysis with Abaqus and FlowVision HPC is based on Abaqus Direct Coupling Interface (DCI) as shown Figure 11 below.

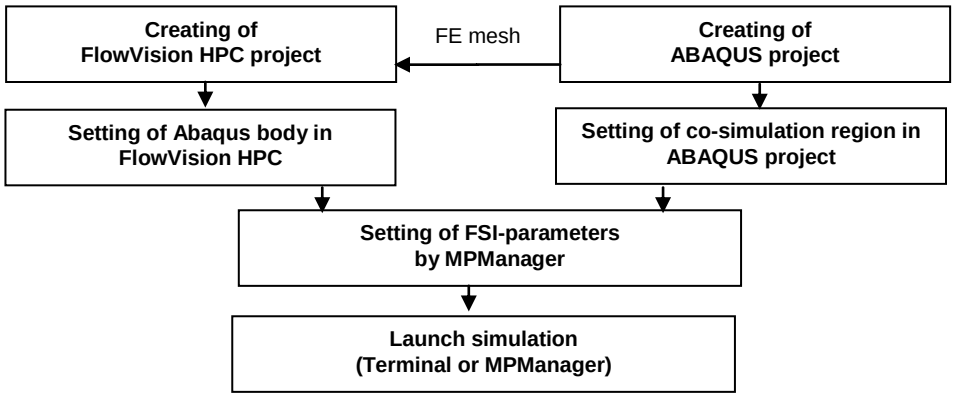

Figure 11. Co-simulation DCI arrangement.

FlowVision is the master application with Abaqus working in slave mode. At each DCI interaction, FlowVision provides Abaqus with the predicted loadings on each plank and outrigger. These loadings are used by Abaqus to compute the displaced nodal coordinates of each part, which are returned to FlowVision for the subsequent time step.

5. Preliminary results from the coupled CFD and structural analyses

The presented results focus on the predicted total lift force generated for a range of flap deflections. Comparisons are then drawn between these results and the predicted lift force versus flap deflection from the concept design study described in section 1.4. Unsteady flow giving rise to oscillating movements of the wing-sail planks, and hence a time dependence of the lift force is also presented.

5.1 Predicted lift force with flap deflection

Several numerical experiments have been carried out for 0, 3, 5, 7 and 8 degrees of upward flap deflection. The typical velocity pattern near the boat and pressure distributions over the surfaces of the boat are shown in Figure 12. Likewise, the predicted relative displacements of each of the wing-sail planks and the outriggers is given in Figure 13 for the case with a fixed flap angle deflection of 8 degrees.

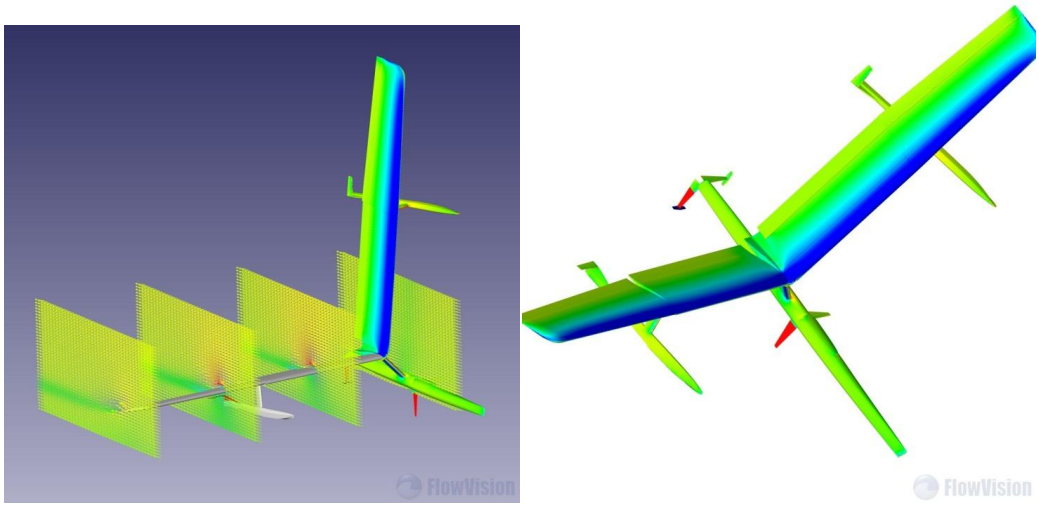

Fig. 12. Distribution of air velocity near wing-sail and pressure over boat surface.

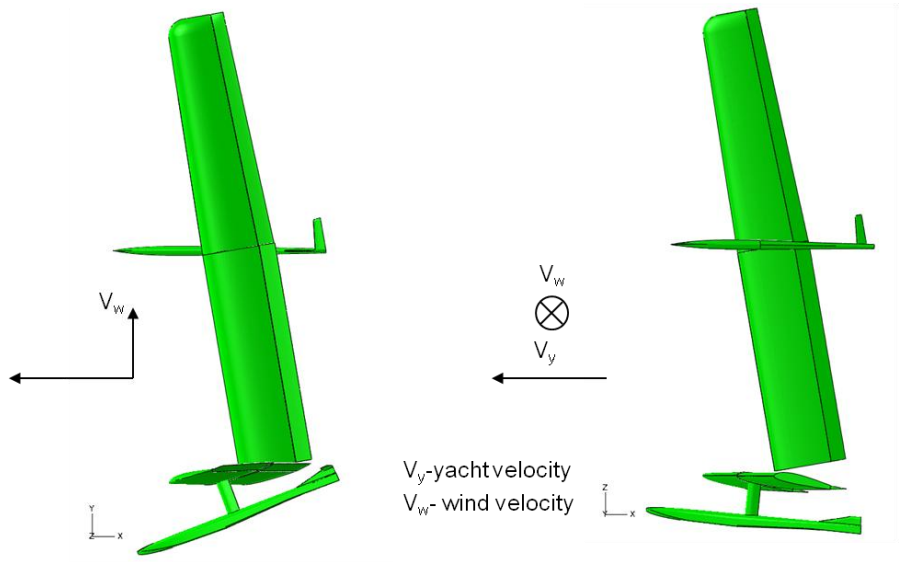

Figure 13. Wing-sail displacements at 8 degrees flap deflection.

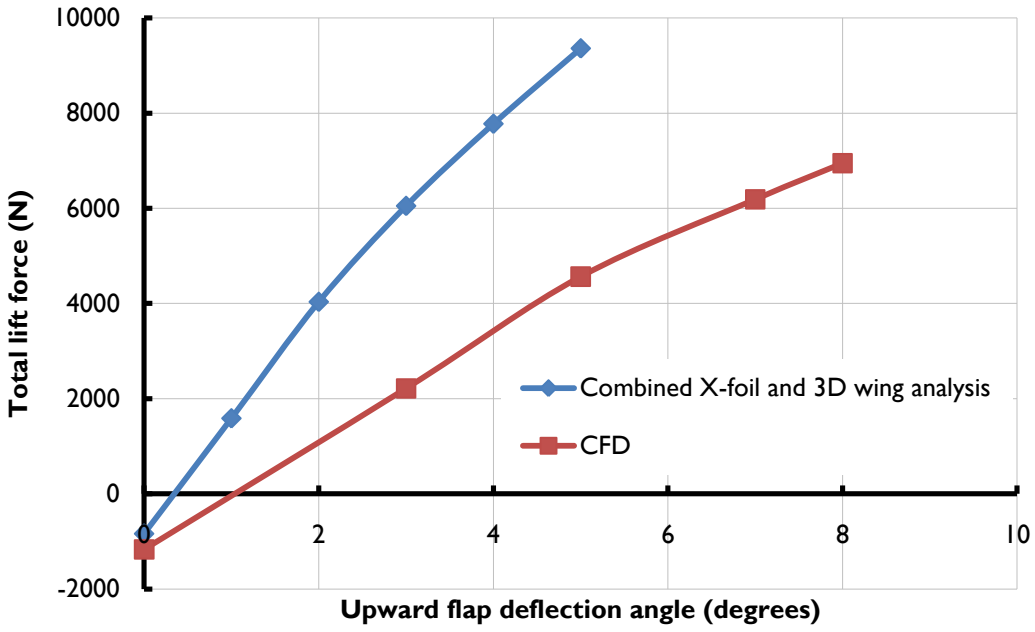

Figure 14. Dependence of wing-sail lift force on angle of flap deflection.

The predicted lift force is presented as a function of flap deflection in Figure 14. For comparison, a similar curve is also presented for the simplified analyses combining X-foil and 3D wing analysis using the discrete vortex Weissinger computation method, which were undertaken at the conceptual design stage. It is apparent that the 3D effects captured within the coupled Abaqus-CFD analyses are important and are manifested as a reduction in lift force for any given flap deflection.

5.2 Time dependence of wing-sail plank displacement and lift force

The predicted time-history of displacement measured at the trailing edge of each flap is presented in Figure 15 for the case with 8 degrees of flap deflection. It is apparent that after a short period, each of the planks is predicted to oscillate about a steady displacement. It is noted that the mean displacement and the frequency of oscillation is generally different for each plank.

The predicted time-history of the lift force for a range of flap angle deflections is given in Figure 16. Similarly, the amplitude of the lift force oscillation with differing flap angles is presented in Figure 17. It is apparent that the amplitude of the lift force oscillation, and the frequency of oscillation, is dependent upon the flap angle deflection at the trailing edge of each wing-sail.

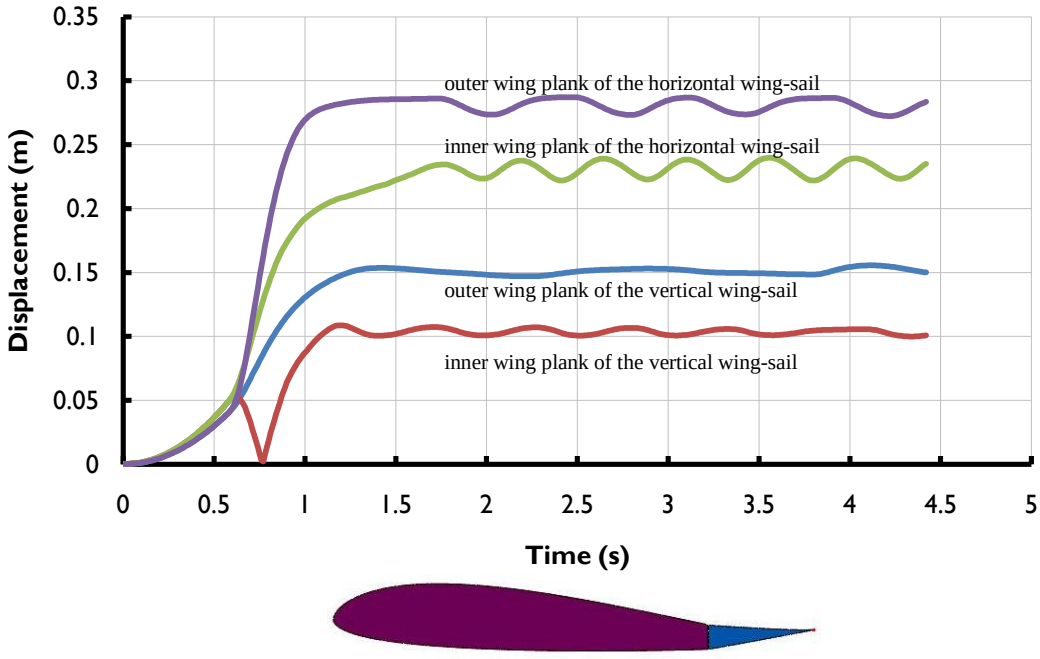

Figure 15. Time dependence of wing-sail plank displacement.

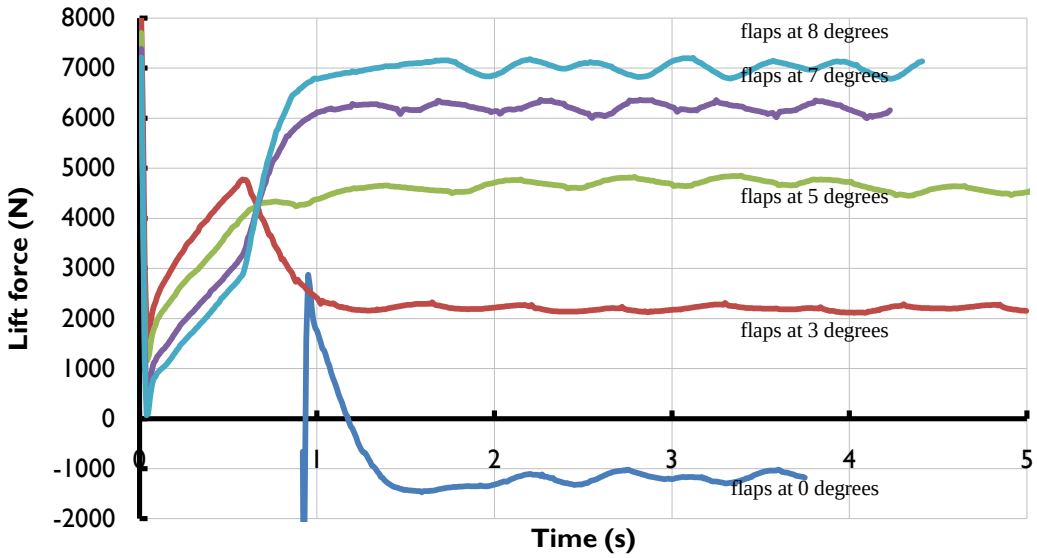

Figure 16. Time dependence of lift force.

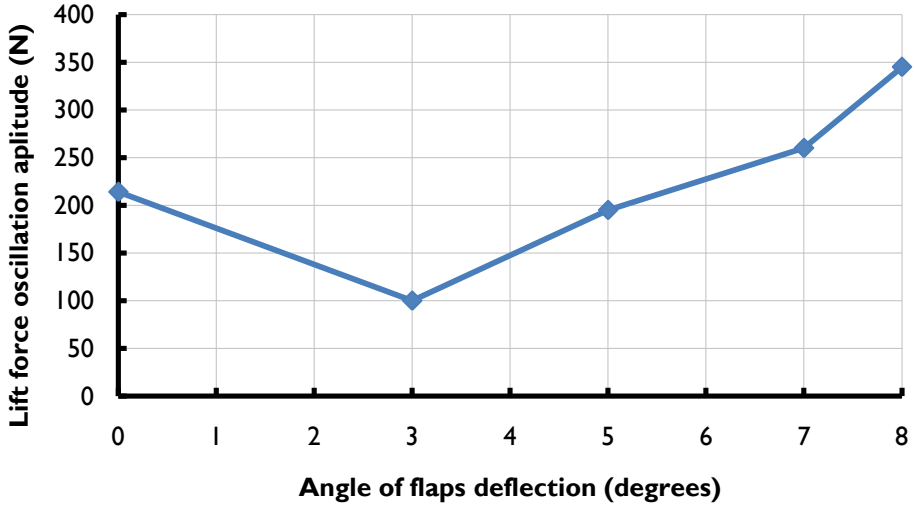

Figure 17. Dependence of amplitude of lift force oscillation upon angle of flap deflection.

6. Conclusions

6.1 Predicted lift force with flap deflection

A comparison between the predicted lift force for a given flap deflection from traditional methods and from CFD is given in Figure 14. Compared to the CFD results, the traditional X-foil/3D wing analysis approach significantly overestimated the degree of lift for a given flap angle deflection. An explanation for this may be that the degree of relative wing sweep angle between the horizontal wing-sail and the apparent wind is reducing the effectiveness of the trailing edge flaps. The relative sweep-back of the horizontal wing-sail will increase the end-effects of each of the planks.

6.2 Predicted time dependence of wing-sail plank displacement and lift force

The predicted oscillations of the wing-sail planks are shown in Figures 15 to 17. These effects may be attributed to reducing stability of the wing-sail planks with increasing effective wing-sweep. This can explain the increased displacement amplitude of the horizontal planks when compared to the vertical planks as shown in Figure 15; the vertical wing-sail has a smaller degree of wing-sweep compared to the horizontal wing-sail. A possible solution may be increasing the static stability of each plank and increasing the effectiveness of the flaps with high effective wing sweep angles.

7. Ongoing work

A simplified FE model of the wing-sails has been constructed and correlated with a detailed FE analysis, in order to give a similar overall structural behavior. This simplified FE model is being used as part of a series of ongoing fluid structure interaction analyses to capture the aerodynamic characteristics of the boat. Such analyses are able to capture deformations along the axis of each of the wing-sails.

The coupled CFD and structural analysis of the entire portion of the boat above the surface will lead to optimizations of the wing-sails. For example, the effect of altering the position of the airfoil axis of rotation and, if necessary, introducing a degree of rotational damping to the movement of each plank, can be assessed. This should lead to the elimination of any tendency for the planks to oscillate. The simulations will enable the rate of movement of each trailing edge flap to be tuned to minimize cross coupling between lift/power (control stick fore/aft movement) and roll (control stick left/right movement). The rate of movement of each flap can also be tuned to maximize power from the wing-sails, whilst maintaining overall roll balance of the boat.

The principle results for each run of the simulation are the resultant forces and moments in relation to a chosen coordinate system. It is intended to run the simulation with several different boat speeds chosen across the boat's speed range. With each run, the trailing edge flaps will be positioned to achieve the necessary degree of lift and roll moment for the pertinent boat speed. The full set of forces and moments generated, together with similar data from the free surface hydrodynamic CFD simulations and foil analyses will be used to generate a final series of mathematical models to build a complete picture of the boat's performance, stability and control. This process will enable optimization of the overall proportions and mass properties of the boat,

including the fore/aft position of the boat centre of gravity, the area and incidence of the horizontal rudder hydrofoil, and the fore/aft position of the keel.

8. References

CLARKE, T., ‘Preliminary design of a composite wing-sail’, Simulia Customer Conference, 2010.